

N92-13955

ANALYSIS AND DESIGN OF TRANSONIC AIRFOILS  
USING STREAMWISE COORDINATES

R.M. BARRON AND C.-F. AN

Department of Mathematics and Statistics  
and Fluid Dynamics Research Institute  
University of Windsor  
Windsor, Ontario, Canada N9B 3P4

Abstract. In this work, a new approach is developed for analysis and design of transonic airfoils. A set of full-potential-equivalent equations in von Mises coordinates is formulated from the Euler equations under the irrotationality and isentropic assumptions. This set is composed of a main equation for the main variable  $y$ , and a secondary equation for the secondary variable  $R$ . The main equation is solved by type-dependent differencing combined with a shock point operator. The secondary equation is solved by marching from a non-characteristic boundary. Sample computations on NACA 0012 and biconvex airfoils show that, for the analysis problem, the present approach achieves good agreement with experimental  $C_p$  distributions. For the design problem, the approach leads to a simple numerical algorithm in which the airfoil contour is calculated as a part of the flow field solution.

1. Introduction

Transonic flow is a widely encountered phenomenon in aeronautics and astronautics but is not easy to calculate because the flow field, and the governing equations as well, are mixed type. Therefore, transonic computation had little progress until 1971 when Murman and Cole developed a type-dependent difference scheme and successfully solved the transonic small disturbance (TSD) equation[1]. Since then, transonic computation has become one of the most upsurging topics for computational fluid dynamicists[2-8]. In 1974, Jameson extended transonic flow computation to the full potential (FP) stage by constructing a rotated difference scheme[4]. Afterwards, papers were published on transonic computation by solving Euler equations[5,6] and their equivalent streamfunction-vorticity formulation[7,8]. Nevertheless, in spite of the recent active efforts on Euler solvers, the full potential calculation is still attractive due to its simplicity, efficiency and sufficient accuracy.

The von Mises transformation is a type of streamline-based transformation which generates a streamwise coordinate system. The von Mises formulation has a number of advantages when applied in CFD. For example, one can resolve the problem of body-fitting coordinates without performing any grid generation. This is because the governing equation (flow physics) and grid generation equation (flow geometry) are combined together in this formulation. Furthermore, the boundary condition on the airfoil for the analysis problem is Dirichlet, and a non-iterative design technique

can be developed for the inverse problem, leading to simplified numerical algorithms and a saving of computer time. Therefore, since Barron[9] connected the von Mises transformation with Martin's approach[10] and solved incompressible 2-D symmetric flow, numerical simulations based on the von Mises transformation have been considerably extended, such as to incompressible lifting[11], axisymmetric[12] and design[13] problems, and to transonic flow[14,15]. In addition, Greywall[16] and Dulikravich[17] obtained a similar formulation for incompressible and compressible flows, respectively.

However, when extending Barron's approach[9] to transonic flow, several problems appear. For compressible flow, apart from the von Mises variable  $y$ , another variable, the density  $\rho$ , must be updated in each iteration. But in the transonic range, the classical difficulty of double value density-massflux relation still exists. Besides, shock waves are not easy to handle in von Mises coordinates either by the artificial density technique or by type-dependent differencing. Recently, the authors[18] developed a new approach to overcome these difficulties by solving so-called full-potential-equivalent equations in von Mises coordinates. The principal advances over the previous transonic work[14,15] are as follows: 1) To update density, instead of solving the non-linear algebraic Bernoulli equation, a first order partial differential equation is solved, thereby avoiding the double density problem; 2) To handle shock waves properly, a shock point operator in von Mises coordinates is proposed and combined with the type-dependent difference scheme so that shock waves can be captured correctly; 3) Introducing a concept of generalized density linearizes the density equation.

In the next section, an outline of the mathematical formulation is given. The numerical algorithms for analysis and design problems are constructed in sections 3 and 4. In section 5, sample computations are performed to test the approach, and conclusions are given in section 6.

## 2. Flow Equations in Streamwise Coordinates

Two dimensional, steady, inviscid fluid flows are governed by the Euler equations

$$\begin{pmatrix} \rho u \\ \rho u^2 + p \\ \rho uv \\ \rho uH \end{pmatrix}_x + \begin{pmatrix} \rho v \\ \rho v^2 + p \\ \rho vH \end{pmatrix}_y = 0 \quad (2-1)$$

where  $\rho$  is density,  $u$  and  $v$  are velocity components in Cartesian coordinates,  $p$  is pressure,  $H = \frac{\gamma}{\gamma-1} p/\rho + (u^2 + v^2)/2$  is total enthalpy and  $\gamma$  is the ratio of specific heats.  $\rho, u, v$  and  $p$  are normalized by free stream density  $\rho_\infty$ , speed  $q_\infty$  and dynamic pressure head  $\rho_\infty q_\infty^2$  while  $x$  and  $y$  are scaled by the airfoil chord length.

Introducing streamfunction  $\psi$ , such that  $\psi_y = \rho u, \psi_x = -\rho v$  and substituting

into equation (2-1), one gets

$$\begin{pmatrix} \psi_y^2/\rho + p \\ -\psi_x\psi_y/\rho \\ \psi_y H \end{pmatrix}_x + \begin{pmatrix} -\psi_x\psi_y/\rho \\ \psi_x^2/\rho + p \\ -\psi_x H \end{pmatrix}_y = 0. \quad (2-2)$$

Streamfunction  $\psi = \psi(x, y)$  can be rewritten in an implicit form,  $F(x, y, \psi) = 0$ , or in an explicit form,  $y = y(x, \psi)$ . This process is equivalent to introducing von Mises transformation:  $x \equiv \phi, y = y(\phi, \psi)$ . If the Jacobian  $J = \partial(x, y)/\partial(\phi, \psi) \neq 0, \infty$ , then the transformation is single-valued and (2-2) becomes

$$\begin{pmatrix} 1/(\rho y_\psi) + p y_\psi \\ y_\phi/(\rho y_\psi) \\ H \end{pmatrix}_\phi + \begin{pmatrix} -p y_\phi \\ p \\ 0 \end{pmatrix}_\psi = 0 \quad (2-3)$$

where the total enthalpy  $H = \frac{\gamma}{\gamma-1} p/\rho + (1 + y_\phi^2)/(2\rho^2 y_\psi^2)$ . The streamline ordinate  $y$ , called von Mises variable, is viewed as a function of  $\phi$  and  $\psi$ . The velocity components can be easily calculated from  $u = 1/(\rho y_\psi), v = y_\phi/(\rho y_\psi)$ , after  $y$  and  $\rho$  are solved.

It is known that the entropy increase across a shock wave is of third order of the shock strength. So, if the shock is not strong, transonic flow can be assumed isentropic and irrotational. Replacing the energy equation in (2-3) by the isentropic relation and keeping in mind that  $\phi \equiv x$ , we reduce (2-3) to

$$\left(\frac{1}{\rho y_\psi} + p y_\psi\right)_x - (p y_x)_\psi = 0, \quad (2-4a)$$

$$\left(\frac{y_x}{\rho y_\psi}\right)_x + p_\psi = 0, \quad (2-4b)$$

$$p = \frac{\rho^\gamma}{\gamma M_\infty^2}, \quad (2-4c)$$

$$\left(\frac{y_x}{\rho}\right)_x - \left(\frac{1 + y_x^2}{\rho y_\psi}\right)_\psi = 0 \quad (2-4d)$$

where  $M_\infty$  is free stream Mach number and the last equation is the irrotationality condition,  $\omega = 0$ , expressed in von Mises coordinates. Substituting (2-4c) into (2-4a) and (2-4b) and expanding (2-4d), we get

$$-y_{x\psi} + y_\psi \left(y_\psi^2 \frac{\rho^{\gamma+1}}{M_\infty^2} - 1\right) \frac{\rho_x}{\rho} - y_x y_\psi^2 \frac{\rho^{\gamma+1}}{M_\infty^2} \frac{\rho_\psi}{\rho} = 0, \quad (2-5a)$$

$$y_\psi y_{xx} - y_x y_{x\psi} - y_x y_\psi \frac{\rho_x}{\rho} + y_\psi^2 \frac{\rho^{\gamma+1}}{M_\infty^2} \frac{\rho_\psi}{\rho} = 0, \quad (2-5b)$$

$$y_\psi^2 y_{xz} - 2y_x y_\psi y_{x\psi} + (1 + y_x^2) y_{\psi\psi} - y_x y_\psi^2 \frac{\rho_x}{\rho} + y_\psi (1 + y_x^2) \frac{\rho_\psi}{\rho} = 0. \quad (2-5c)$$

Properly manipulating the above three equations can produce several sets of equations. Each set has two independent equations for two variables. To make the formulation more compact, define generalized density  $R = \rho^{\gamma+1}$  as an alternative to density  $\rho$ . Solving for  $\rho_x/\rho$  and  $\rho_\psi/\rho$  from (2-5a) and (2-5b), and substituting into (2-5c), one gets

$$(y_\psi^2 - \frac{M_\infty^2}{R}) y_{xz} - 2y_x y_\psi y_{x\psi} + (1 + y_x^2) y_{\psi\psi} = 0. \quad (2-6a)$$

Eliminating  $y_{x\psi}$  from (2-5a) and (2-5b) gives

$$y_x y_\psi^2 R_x - y_\psi (1 + y_x^2) R_\psi = (\gamma + 1) M_\infty^2 y_{xz}. \quad (2-6b)$$

Equation (2-5a) can be rewritten as

$$y_\psi (y_\psi^2 - \frac{M_\infty^2}{R}) R_x - y_x y_\psi^2 R_\psi = (\gamma + 1) M_\infty^2 y_{x\psi}. \quad (2-6c)$$

Substituting the above  $y_{xz}$ ,  $y_{x\psi}$  into (2-5c) and replacing  $\rho$  by  $R$ , one obtains

$$y_x (y_\psi^2 - \frac{M_\infty^2}{R}) R_x + y_\psi (1 - y_x^2 - \frac{M_\infty^2}{R} \frac{1 + y_x^2}{y_\psi^2}) R_\psi = (\gamma + 1) M_\infty^2 \frac{1 + y_x^2}{y_\psi^2} y_{\psi\psi}. \quad (2-6d)$$

It is important to note that (2-6b) is linear after introducing the new variable  $R$ . The term  $M_\infty^2/R$  is usually called compressibility factor.

In principle, any two of the above four equations could be combined as a set of equations to solve for  $y$  and  $R$ . But, in practice, equation (2-6a) is always selected to solve for  $y$  and one of the remaining three equations is selected to solve for  $R$ . Equation (2-6a) is a second order, non-linear, partial differential equation of mixed type depending on the local flow property. If the flow is subsonic/supersonic, then (2-6a) is elliptic/hyperbolic. In other words, the mathematical classification of the equation is consistent with the physical nature of the local flow. Therefore, (2-6a) is named the main equation for the corresponding main variable  $y$ . Equations (2-6b) - (2-6d) are called secondary equations for the secondary variable  $R$ . Among the three secondary equations, (2-6b) appears simpler because it is linear and hence priority is given to it to accompany the main equation. The main equation (2-6a) and one of the secondary equations (2-6b) - (2-6d) constitute a set of so-called full-potential-equivalent equations. They are coupled with each other and solved in an alternating and iterative manner. More details and other forms of full-potential-equivalent equations can be found in [18].

### 3. Analysis Problem

For a symmetric airfoil placed in a transonic stream at zero angle of attack, the governing equations (2 - 6a) and (2 - 6b) can be rewritten as

$$A_1 y_{xx} + A_2 y_x \psi + A_3 y_{\psi\psi} = 0, \quad (3-1)$$

$$B_1 R_x + B_2 R_\psi = B_3 \quad (3-2)$$

where  $A_1 = y_\psi^2 - M_\infty^2/R$ ,  $A_2 = -2y_x y_\psi$ ,  $A_3 = 1 + y_x^2$ ,  $B_1 = y_x y_\psi^2$ ,  $B_2 = -y_\psi(1 + y_x^2)$ ,  $B_3 = (\gamma + 1)M_\infty^2 y_{xx}$ . The boundary conditions on  $y$  are Dirichlet:  $y = f(x)$  on the airfoil,  $y = \psi$  at infinity,  $y = 0$  on the symmetry line and  $R = 1$  at infinity, where  $f(x)$  is the airfoil shape function. The computational domain and boundary conditions are shown in Fig.1.

Since the mathematical character of (3 - 1) depends on the local flow property, it is necessary to apply Murman and Cole's type-dependent scheme[1] to solve for  $y$ . Applying the type-dependent difference scheme to (3 - 1) gives

$$A y_{i,j-1} + B y_{i,j} + C y_{i,j+1} = RHS \quad (3-3)$$

where  $A = \beta^2 A_3 - \frac{1-\nu}{2} \beta A_2$ ,  $B = -2\beta^2 A_3 + (1 - 3\nu)A_1$ ,  $C = \beta^2 A_3 + \frac{1-\nu}{2} \beta A_2$ ,

$$\begin{aligned} RHS = & -\nu A_1 (y_{i+1,j} + y_{i-1,j}) + (1 - \nu) A_1 (2y_{i-1,j} - y_{i-2,j}) \\ & - \nu \beta A_2 (y_{i+1,j+1} - y_{i+1,j-1} - y_{i-1,j+1} + y_{i-1,j-1})/4 \\ & + (1 - \nu) \beta A_2 (y_{i-1,j+1} - y_{i-1,j-1})/2, \end{aligned}$$

and  $\beta = \Delta x / \Delta \psi$ , for  $i = 2, 3, \dots, I_{max} - 1$ ,  $j = 2, 3, \dots, J_{max} - 1$ . The switch parameter  $\nu = 1$  for a subsonic point,  $\nu = 0$  for a supersonic point. The resulting system of difference equations (3 - 3) has a tridiagonal coefficient matrix so that SLOR can be applied by relaxing along vertical lines, sweeping from left to right and iterating up to convergence. (see Fig.1)

After  $y(x, \psi)$  is solved from the main equation (3 - 1) and  $y_x, y_\psi, y_{xx}$  are properly differenced, the secondary equation (3 - 2) can be solved for  $R(x, \psi)$  by marching from an initial line other than its characteristic curve. The slope of its characteristic curve is  $d\psi/dx = -(1 + y_x^2)/(y_x y_\psi)$ . At infinity,  $d\psi/dx = \infty$ . Thus, left and right far field boundaries are characteristic curves and hence cannot serve as initial lines. Fortunately, the horizontal boundary is not a characteristic and we can march equation (3 - 2) from the top boundary to the airfoil using the condition  $R = 1$  at infinity.

The Crank-Nicolson scheme for (3 - 2) gives

$$\tilde{A} R_{i-1,j} + \tilde{B} R_{i,j} + \tilde{C} R_{i+1,j} = \tilde{RHS} \quad (3-4)$$

where  $\widetilde{RHS} = \widetilde{C}R_{i-1,j+1} + \widetilde{B}R_{i,j+1} + \widetilde{A}R_{i+1,j+1} + 4\Delta x B_3$ ,  $\widetilde{A} = -B_1$ ,  $\widetilde{B} = -4\beta B_2$ ,  $\widetilde{C} = B_1$ ,  $\beta = \Delta x / \Delta \psi$  for  $j = J_{max} - 1, \dots, 3, 2, 1$ ,  $i = 2, 3, \dots, I_{max} - 1$ . The system of difference equations (3-4) can be solved row by row from the horizontal far field to the airfoil using SLOR, but no iteration is needed because (3-2) is linear. After  $R$  is solved, the pressure coefficient is calculated from

$$C_p = \frac{2}{\gamma M_\infty^2} (R^{\frac{\gamma}{\gamma-1}} - 1). \quad (3-5)$$

However, it has been found after numerical tests that this procedure is efficient only for flow in which the shock is weak. For flow with a stronger shock, the iterations fail to converge. To overcome this difficulty, a special treatment of the shock wave is proposed following the ideas of Murman's shock structure analysis[2,3]. For usual transonic flows, the shock wave is approximately normal and the shock jump conditions are given by

$$\left[ \frac{y_x}{\rho} \right] = 0, \quad [y_\psi] = 0. \quad (3-6)$$

where [...] represents a jump across the shock. Based on this analysis, the difference quotient approximations to  $y_{xx}$ ,  $y_{x\psi}$  at a shock point, i.e. grid point just behind the shock, are constructed as below:

$$(y_{xx})_{i,j} = \frac{1}{\Delta x^2} (y_{i+1,j} - y_{i,j} - \alpha_j y_{i-1,j} + \alpha_j y_{i-2,j}) \quad (3-7a)$$

$$(y_{x\psi})_{i,j} = \frac{1}{4\Delta x \Delta \psi} (y_{i+1,j+1} - y_{i+1,j-1} + y_{i,j+1} - y_{i,j-1} - 3y_{i-1,j+1} + 3y_{i-1,j-1} + y_{i-2,j+1} - y_{i-2,j-1}). \quad (3-7b)$$

where  $\alpha_j$  is the density jump factor on  $j^{\text{th}}$  streamline and given by the Rankine-Hugoniot relation of a normal shock. (3-7a) and (3-7b) are called shock point operator (SPO) in von Mises coordinates. The difference equations (3-3) for  $y$  and (3-4) for  $R$  are modified using SPO. Numerical experimentation has shown that SPO must be applied in the  $y_{xx}$ ,  $y_{x\psi}$  terms of the main equation (3-1) and in the  $B_3$  term of the secondary equation (3-2). SPO is a crucial tool to capture shock waves in supercritical transonic flows.

#### 4. Design Problem

Similar to the analysis problem, the main equation (2-6a) and secondary equations (2-6b) or (2-6c) can be solved for  $y$  and  $R$  alternatively:

$$A_1 y_{xx} + A_2 y_{x\psi} + A_3 y_{\psi\psi} = 0, \quad (4-1a)$$

$$B_1 R_x + B_2 R_\psi = B_3, \quad (4-1b)$$

$$D_1 R_x + D_2 R_\psi = D_3 \quad (4-1c)$$

where  $A_1 = y_\psi^2 - M_\infty^2/R$ ,  $A_2 = -2y_x y_\psi$ ,  $A_3 = 1 + y_x^2$ ,  $B_1 = y_x y_\psi^2$ ,  $B_2 = -y_\psi(1 + y_x^2)$ ,  $B_3 = (\gamma + 1)M_\infty^2 y_{xx}$ ,  $D_1 = y_\psi(y_\psi^2 - M_\infty^2/R)$ ,  $D_2 = -y_x y_\psi^2$ ,  $D_3 = (\gamma + 1)M_\infty^2 y_{x\psi}$ . The boundary conditions are the same as in the analysis problem, except on the airfoil, which is unknown. There, the pressure coefficient  $C_{p_s}$  is specified, hence, the generalized density is also specified:

$$R_s = (1 + \gamma M_\infty^2 C_{p_s} / 2)^{(\gamma+1)/\gamma} \quad (4-2)$$

On the airfoil surface, the Bernoulli equation in von Mises coordinates leads to

$$F(x)y_\psi^2 - y_x^2 = 1 \quad (4-3)$$

where

$$F(x) = \frac{2}{(\gamma - 1)M_\infty^2} \left[ \left(1 + \frac{\gamma - 1}{2} M_\infty^2\right) R_s^{\frac{2}{\gamma+1}} - R_s \right].$$

This is a Neumann boundary condition on the airfoil when solving (4-1a) for  $y$ . (4-2) is a Dirichlet boundary condition on the airfoil when solving (4-1c) for  $R$ . In addition, on a symmetry line off the airfoil,  $R_\psi = 0$ .

If streamlines do not intersect each other on the airfoil, then  $y_\psi > 0$ , and if, furthermore,  $F(x) \neq 0$  on the airfoil, then equation (4-3) gives  $y_\psi = \sqrt{(1 + y_x^2)/F(x)}$ . For most practical transonic flows the required conditions are easily satisfied as long as  $C_{p_s}$  is reasonably specified. Differencing  $y_\psi$ , we get

$$y_{i,1} = [4y_{i,2} - y_{i,3} - 2G(x_i)]/3 \quad (4-4)$$

where  $G(x_i) = \Delta\psi \sqrt{[1 + (y_x^2)_{i,1}]/F(x_i)}$ . Considering this new boundary condition, we modify system (3-3) as follows:

For  $j = 2$ , equation (3-3) reads  $Ay_{i,1} + By_{i,2} + Cy_{i,3} = RHS$ . Substituting (4-4) into it, we have

$$(B + 4A/3)y_{i,2} + (C - A/3)y_{i,3} = RHS + 2AG(x_i)/3 \quad (4-5)$$

Replacing the first equation in system (3-3) by (4-5), solving the resulting system and applying (4-4), we can obtain the desired airfoil contour  $f(x_i) = y_{i,1}$  without further iteration of the airfoil shape. The computational domain and boundary conditions are shown in Fig. 2.

To solve for the secondary variable  $R$ , two secondary equations (4-1b) and (4-1c) are available. For equation (4-1b), the marching procedure is the same as in the analysis problem, while for equation (4-1c), the marching procedure is

different. The slope of its characteristic curve is  $d\psi/dx = -(y_x y_\psi)/(y_\psi^2 - M_\infty^2/R)$ . At infinity,  $d\psi/dx = 0$ . So, the horizontal far field boundary is a characteristic curve, but the vertical boundaries are not. Therefore, the marching process can be carried out from left to right.

Crank-Nicolson scheme for (4-1c) gives

$$\bar{A}R_{i,j-1} + \bar{B}R_{i,j} + \bar{C}R_{i,j+1} = R\bar{H}S \quad (4-6)$$

where  $R\bar{H}S = \bar{C}R_{i-1,j-1} + \bar{B}R_{i-1,j} + \bar{A}R_{i-1,j+1} + 4\Delta x D_3$ ,  $\bar{A} = -\beta D_2$ ,  $\bar{B} = 4D_1$ ,  $\bar{C} = \beta D_2$ ,  $\beta = \Delta x/\Delta\psi$ , for  $i = 2, 3, \dots, I_{max} - 1$ ,  $j = 2, 3, \dots, J_{max} - 1$ .

For the first equation in system (4-6), the boundary conditions  $R_{i,1} = R_s(x_i)$  on the airfoil and  $R_{i,1} = R_{i,2}$  on symmetry line should be imposed. It is noted that  $y_x y_\psi$  in  $D_3$  should be type-dependent differenced with SPO to keep consistency with the main equation.

Both (4-1b) and (4-1c) have been coupled with (4-1a). Numerical experiments have shown that (4-1c) gives better accuracy than (4-1b). This is reasonable because the boundary condition on the airfoil is considered not only in the main equation (4-1a), but also in the secondary equation (4-1c), while it is not suitably considered in the secondary equation (4-1b). However, the price to pay is more iterations because (4-1c) is non-linear.

## 5. Sample Computations

The approach developed here is applied to calculated transonic flows for both analysis and design problems. Only symmetric airfoils at zero angle of attack are considered, but both subcritical and supercritical Mach numbers are included. In the computational domain, a 65x33 uniform mesh covers  $-2 \leq x \leq 3$ ,  $0 \leq \psi \leq 2.5$  and the airfoil is placed between 0 and 1. For higher Mach numbers, a 80x31 mesh has been used. The computational domain and boundary conditions are shown in Figures 1 and 2.

Figures 3 and 4 are comparisons of calculated  $C_p$  distributions of NACA 0012 with experimental data at NAE[19] for  $M_\infty = 0.490$  and at ONERA[19] for  $M_\infty = 0.803$ . Figure 5 indicates the calculated  $C_p$  distribution of a 6 percent biconvex airfoil at  $M_\infty = 0.909$  compared with experimental data at NASA[20]. From these plots we can see that the present approach is able to accurately predict  $C_p$  distributions on airfoils in transonic flows. The agreement between computed pressure and available experimental data is quite satisfactory. For supercritical transonic flows, the shock wave can be captured by the presently proposed type-dependent scheme with SPO.

Figure 6 shows the designed contour of a 6 percent biconvex airfoil compared with the exact shape[21]. The specified  $C_p$  distribution on the airfoil comes from experiments at NASA[20] for  $M_\infty = 0.909$ . Figures 7 and 8 give designed NACA 0012 contours compared with the exact shape[21]. The specified  $C_p$  is from NAE[19] for  $M_\infty = 0.490$  and ONERA[19] for  $M_\infty = 0.803$ . Here, we can see that the present approach is capable of designing airfoil contours with satisfactory accuracy.

## 6. Conclusions

1) The newly developed approach based on the full-potential-equivalent equations in von Mises coordinates is able to solve transonic flows for both analysis and design problems.

2) The full-potential-equivalent equations are composed of a main equation for the corresponding main variable, streamline ordinate  $y$ , and a secondary equation for the related secondary variable, generalized density  $R$ .

3) The type-dependent difference scheme with shock point operator is effective to solve the main equation for  $y$  and the shock point operator is crucial to capture shock waves in supercritical transonic flows.

4) The secondary equation can be solved for  $R$  by marching from a certain non-characteristic, density-specified boundary. Crank-Nicolson scheme proves to be useful to march such a equation.

5) For analysis problems, the boundary condition on the airfoil is Dirichlet, which is easy to implement.

6) For design problems, the airfoil contour can be obtained in a non-iterative manner because it is a part of the solution of the main equation.

## References

1. E. M. Murman and J. D. Cole, Calculation of Plane Steady Transonic Flows, AIAA J., Vol.9, 114-121 (1971)
2. E. M. Murman and J. A. Krupp, Solution of the Transonic Potential Equation Using a Mixed Finite Difference System, Lecture Notes in Physics, Vol.8, pp199-206, Springer-Verlag, Berlin, 1974
3. E. M. Murman, Analysis of Embedded Shock Waves Calculated by Relaxation Methods, AIAA J., Vol.12, 626-633 (1974)
4. A. Jameson, Iterative Solution of Transonic Flows over Airfoils and Wings, Including Flows at Mach 1, Communications on Pure and Applied Mathematics, Vol.27, 283-309 (1974)
5. R. M. Beam and R. F. Warming, An Implicit Finite Difference Algorithm for Hyperbolic System in Conservation Law Form, J. of Comp. Phys., Vol.22, 87-110 (1976)
6. J. C. Steger, Implicit Finite Difference Simulation of Flow around Arbitrary Two Dimensional Geometries, AIAA J., Vol.16, 676-686 (1978)
7. M. Hafez and D. Lovell, Numerical Solution of Transonic Stream Function Equation, AIAA J., Vol.21, 327-335 (1983)
8. H. L. Atkins and H. A. Hassan, A New Stream Function Formulation for the Steady Euler Equations, AIAA J., Vol.23, 701-706 (1985)
9. R. M. Barron, Computation of Incompressible Potential Flow Using von Mises Coordinates, J. of Math. and Comp. in Simulation, Vol.31, 177-188 (1989)

10. M. H. Martin, The Flow of a Viscous Fluid I, Archives for Rational Mechanics and Analysis, Vol.41, 266-286 (1971)
11. R. K. Naeem and R. M. Barron, Lifting Airfoil Calculations Using von Mises Variables, Communications in Applied Numerical Methods, Vol. 5, 203-210(1989)
12. R. M. Barron, S. Zhang, A. Chandna and N. Rudraiah, Axisymmetric Potential Flow Calculations, Part 1: Analysis Mode, Communications in Applied Numerical Methods, Vol. 6, 437-445(1990)
13. R. M. Barron, A Non-Iterative Technique for Design of Aerofoils in Incompressible Potential Flow, Communications in Applied Numerical Methods, Vol. 6, 557-564(1990)
14. R. M. Barron and R. K. Naeem, Numerical Solution of Transonic Flows on a Streamfunction Coordinate System, Intl. J. for Num. Methods in Fluids, Vol.9, 1183-1193 (1989)
15. R. K. Naeem and R. M. Barron, Transonic Computations on a Natural Grid, AIAA J., Vol.28, 1836-1838(1990)
16. M. S. Greywall, Streamwise Computation of 2-D Incompressible Potential Flows, J. of Comp. Phys., Vol.59, 224-231 (1985)
17. G. S. Dulikravich, A Stream-Function-Coordinate (SFC) Concept in Aerodynamic Shape Design, AGARD VKI Lecture Series, May 14-18, 1990
18. C.-F. An and R. M. Barron, Numerical Solution of Transonic Full-Potential-Equivalent Equations in von Mises Coordinates, to appear
19. J. J. Thibert, M. Grandjacques and L. H. Ohman, Experimental Data Base for Computer Program Assessment, AGARD AR-138, pp.A1-1 — A1-36, 1979
20. E. D. Knetchtel, Experimental Investigation at Transonic Speeds of Pressure Distributions over Wedge and Circular-Arc-Airfoil Sections and Evaluation of Perforated Wall Interference, NASA TN D-15, 1959
21. I. Abbott and A. E. von Doenhoff, Theory of Airfoil Section, Dover Publ. Inc., N.Y., 1959

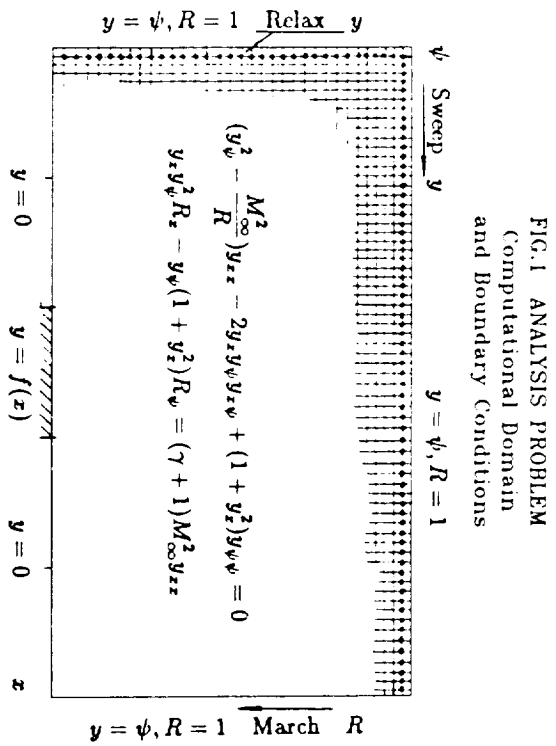


FIG.1 ANALYSIS PROBLEM  
Computational Domain and Boundary Conditions

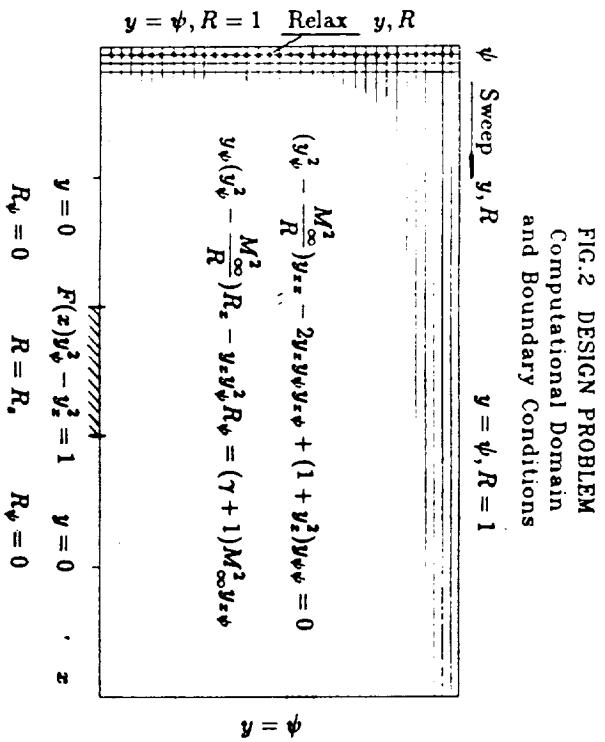


FIG.2 DESIGN PROBLEM  
Computational Domain and Boundary Conditions

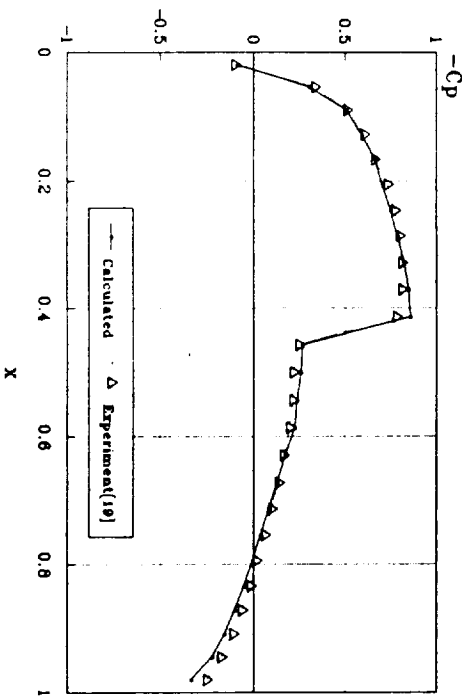
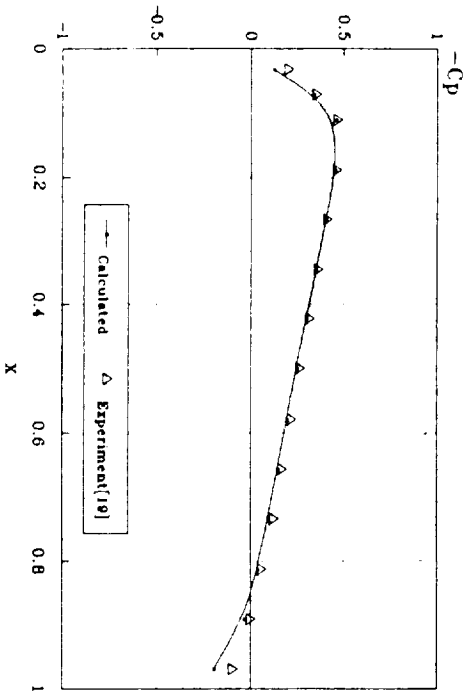


FIG.4 COMPARISON OF Cp DISTRIBUTION  
NACA 0012, Mach=0.803

FIG.5 COMPARISON OF  $C_p$  DISTRIBUTION  
Biconvex(6%) Airfoil, Mach=0.909

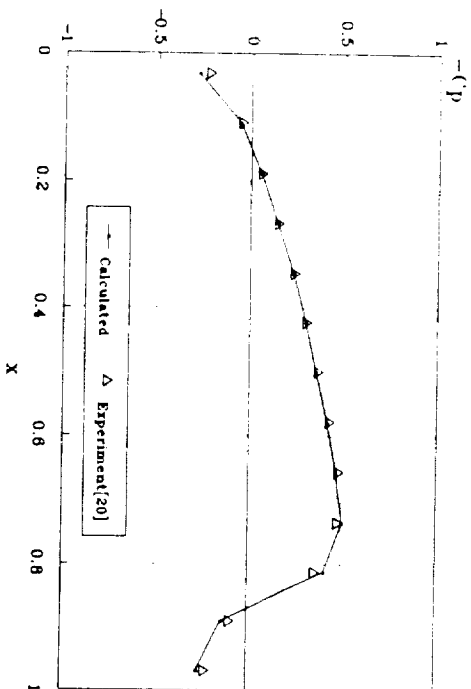


FIG.6 DESIGNED BICONVEX(6%) AIRFOIL  
Mach=0.909

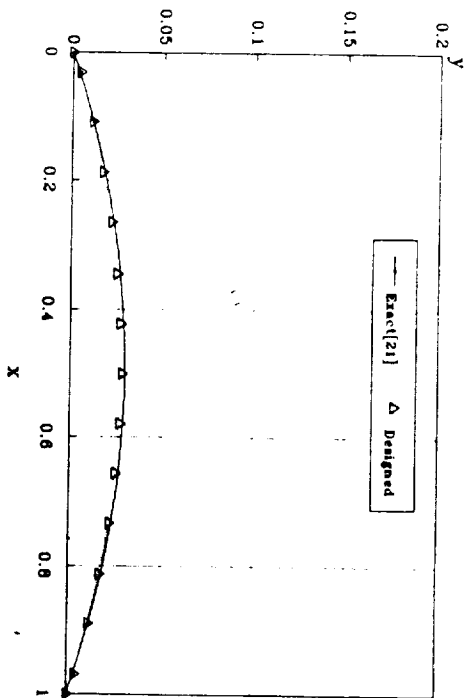


FIG.7 DESIGNED NACA 0012 AIRFOIL  
Mach=0.490

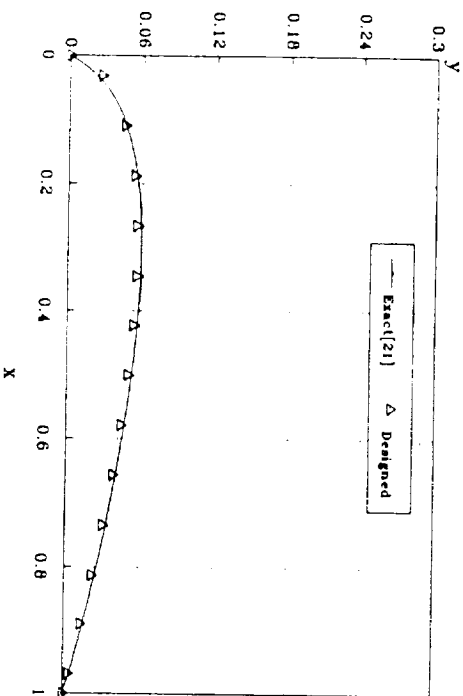


FIG.8 DESIGNED NACA 0012 AIRFOIL  
Mach=0.803

